

Quantum vacuum of strongly nonlinear lattices

O. V. Zhirov,¹ A. S. Pikovsky,² and D. L. Shepelyansky³

¹Budker Institute of Nuclear Physics, Novosibirsk 630090, Russia

²Department of Physics and Astronomy, Potsdam University, Karl-Liebknecht-Strasse 24, D-14476, Potsdam-Golm, Germany

³Laboratoire de Physique Théorique du CNRS (IRSAMC), Université de Toulouse, UPS, F-31062 Toulouse, France

(Received 5 May 2010; revised manuscript received 4 October 2010; published 3 January 2011)

We study the properties of classical and quantum strongly nonlinear chains by means of extensive numerical simulations. Due to strong nonlinearity, the classical dynamics of such chains remains chaotic at arbitrarily low energies. We show that the collective excitations of classical chains are described by sound waves whose decay rate scales algebraically with the wave number with a generic exponent value. The properties of the quantum chains are studied by the quantum Monte Carlo method and it is found that the low-energy excitations are well described by effective phonon modes with the sound velocity dependent on an effective Planck constant. Our results show that at low energies the quantum effects lead to a suppression of chaos and drive the system to a quasi-integrable regime of effective phonon modes.

DOI: 10.1103/PhysRevE.83.016202

PACS number(s): 05.45.-a, 63.20.Ry, 45.50.Jf

I. INTRODUCTION

The investigation of classical nonlinear chains, started by Fermi, Pasta, and Ulam in 1955 [1], still remains an active and interesting area of research which attracts the significant interest of the nonlinear community (see, e.g., Refs. [2–5] and references therein). Usually, in such chains the nonlinear terms are relatively weak compared to the linear ones and strong nonlinear effects appear only at sufficiently high-energy excitations.

However, there are also other types of chains where the linear modes are absent and the dynamics is strongly nonlinear at arbitrarily small energies [6,7]. In some situations, time in such chains can be rescaled with energy and hence the system always remains in a strongly nonlinear regime. A prominent example is the Hertz lattice which describes elastically interacting hard balls. A well-known example of such a system is the toy “Newton’s cradle,” which, however, is typically rather short; in specially assigned experiments one can study long chains of balls where the elasticity parameter scales as a square-root of the displacement [8–11] corresponding to the nonlinearity index $n = 5/2$ of the interaction term in the Hamiltonian. Nesterenko [8,12–14] described a compact traveling-wave solution in the Hertz lattice now known as compacton (for another realization of “Newton’s cradle” in a chain of interacting solitons see Ref. [15]). A rigorous mathematical description of compactons was given by Rosenau and Hyman [16,17] for a class of nonlinear partial differential equations (PDE’s) with nonlinear dispersion. A detailed analysis of the dynamics on lattices with various nonlinearity index has been performed recently in Ref. [18]. On a finite lattice one typically observes chaotic dynamics characterized by a spectrum of positive Lyapunov exponents [18,19].

In the strongly nonlinear lattices the dynamics is typically chaotic at arbitrarily small energies. Therefore it is interesting to understand what happens in such *quantum* lattices, where in the classical limit normal phonon modes are absent and one cannot quantize the system based on phonon representation. To solve the problem, we use the quantum Monte Carlo (QMC) method and the approach developed recently for

the quantum Frenkel-Kontorova model as it is described in Ref. [20]. *The aim of this work is to understand the properties of quantum vacuum and low-energy excitations in lattices with a strongly nonlinear interaction between particles.* It is interesting to note that the recent progress with cold atoms allowed to realize a quantum “Newton’s cradle” [21] and to study energy redistribution between atoms. The experimental progress stimulated also theoretical studies of the integrability and nonintegrability in one-dimensional atomic lattices at high-energy excitations [22]. In contrast to that we study the properties of quantum vacuum and low-energy excitations in quantum lattices when the linear terms are absent and nonlinearity is always strong in the classical case. Thus the classical dynamics of such chains is always chaotic [18] (except a special case of one compacton moving in a lattice) and their quantization is a quite nontrivial task. Due to this it is not possible to apply the ideas of semiclassical quantization in the sense of the classical Gutzwiller’s approach [23] as it has been recently done for breathers [24] and solitons [25].

While the model we study is an ideal one-dimensional lattice that, at first glance, looks rather abstract, a recent experimental progress allows us to look optimistically on the possible experimental realizations (e.g., the quasi-one-dimensional Wigner crystal composed of charged ions confined in a linear Paul or Penning trap as an experimentally accessible situation). We refer to recent papers [26,27] where quantum dynamics of structural defects (kinks) in such configurations have been discussed; see also a suggestion to effectively simulate nonlinear lattice models with ion traps [28]. Another class of experimental situations where such a nonlinear lattice can be realized deliver nanomechanical systems, having in the classical description a large variety of nonlinear properties [29]. The quantum limit of such systems has been reached experimentally quite recently [30].

The paper is organized as follows. The model description is given in Sec. II. The properties of sound-like waves in the classical strongly chains are analyzed in Sec. III. Simple analytical estimates for the strongly nonlinear chain are presented in Sec. IV. Numerical results of the QMC are presented in Sec. V and the results are summarized in Sec. VI.

II. MODEL DESCRIPTION

The quantum strongly nonlinear chain is described by the Hamiltonian

$$\hat{H} = \sum_{l=1}^N \frac{1}{2} \hat{p}_l^2 + \frac{\alpha}{n} (\hat{x}_l - \hat{x}_{l-1})^n, \quad (1)$$

where index l marks the particles in the chain and n is the nonlinearity index. Here x_l gives the particle coordinate counted from the equilibrium distance between particles, which is taken to be a . For the chain of balls like Newton's cradle a is given by the ball diameter (we stress here that we consider the potential acting both for compression and stretching, while in the real chain of balls the force appears only due to compression). We use the dimensionless units in which the particle mass is equal to unity and the momentum p_l gives the particle velocity. For the quantum problem the operators of momentum and coordinate have the usual commutator $[\hat{p}_l, \hat{x}_{l'}] = -i\hbar\delta_{l,l'}$ with a dimensionless Planck constant \hbar . Here and in the following we use the fixed boundary conditions with $x_{l=0} = x_{l=N} = 0$. We note that the particles are distinguishable since they are located at well-defined positions.

Let us recall a few known results for the harmonic chain at $n = 2$. It is convenient to introduce sine modes via relations $\hat{S}_k = \sqrt{\frac{2}{N}} \sum_l \sin(q_k l) \hat{x}_l$, $\hat{x}_l = \sqrt{\frac{2}{N}} \sum_k \sin(q_k l) \hat{S}_k$ and the corresponding relation for momenta. Then the Hamiltonian (1) takes the form

$$\hat{H} = \frac{1}{2} \sum_k (\hat{P}_k^2 + \omega_k^2 \hat{Q}_k^2), \quad (2)$$

with the normal mode frequencies $\omega_k = 2\bar{\omega} \sin(q_k/2)$, $\bar{\omega} = \sqrt{\alpha}$ and wave numbers $q_k = \pi k/N$, $k = 1, \dots, N-1$.

The quantum vacuum state of the chain is a product of quantum vacuum states of all modes. For any mode in the quantum vacuum state one has an average of mode energy \hat{U}_k being $\langle \hat{U}_k \rangle = \omega_k^2 \langle \hat{S}_k^2 \rangle / 2 = \hbar\omega_k / 4$ and hence

$$\langle \hat{S}_k \hat{S}_{k'} \rangle = \frac{\hbar}{2\omega_k} \delta_{kk'}. \quad (3)$$

Different modes are independent and as a result the squared deviation from equilibrium for a particle l is $\langle \hat{x}_l^2 \rangle = \frac{2}{N} \sum_{k=1}^{N-1} \sin^2(q_k l) \langle \hat{S}_k^2 \rangle = \frac{\hbar}{N} \sum_{k=1}^{N-1} \sin^2(q_k l) / \omega_k$. For the central particle $l = N/2$, the displacement diverges logarithmically with the chain length $\langle \hat{x}_l^2 \rangle = \frac{\hbar}{4\pi} \sum_{k=1}^{N-1} 1/\sin(q_k/2) \approx \frac{\hbar}{\pi} \ln(2/q_{\min})$, where $q_{\min} \equiv q_{k=1} = \pi/N$. For $\hbar = 1$ the displacement is of the order of unity for $N \sim 30$. We will assume that such displacements are small compared to the distance a between particles.

The spacial correlator of the chain can be also explicitly calculated as $\langle \hat{x}_l \hat{x}_{l+\Delta} \rangle = \frac{2}{N} \sum_{k=1}^{N-1} \sin(q_k l) \sin(q_k(l+\Delta)) \langle \hat{S}_k^2 \rangle$, where the brackets note the quantum average. Using Eq. (3) we obtain after summation over all l

$$\langle \hat{x}_l \hat{x}_{l+\Delta} \rangle_l \approx \frac{\hbar}{N} \sum_{k=1}^{N-1} \frac{\cos(q_k \Delta)}{4 \sin(q_k/2)}. \quad (4)$$

At finite temperature T the relation (3) is modified for the usual expression for bosons

$$\langle \hat{S}_k^2 \rangle = \frac{\hbar}{\omega_k} \left(\frac{1}{2} + \frac{1}{\exp(\hbar\omega_k/T) - 1} \right). \quad (5)$$

With this form of $\langle \hat{S}_k^2 \rangle$ one can obtain the expression for the correlator $\langle \hat{x}_l \hat{x}_{l+\Delta} \rangle$ at finite temperature.

The properties of the chain can be also characterized by the static form factor defined as

$$F(q) = \left| \left\langle \sum_l \exp[i(a \cdot l + \hat{x}_l)q/\hbar] \right\rangle \right|^2, \quad (6)$$

where q can be viewed as a momentum transfer during a process of photon scattering, and a is the spacing of the chain lattice.

Before starting the studies of the quantum problem at $n > 2$, we consider in the next section the features of the classical chain at $n = 4$ and finite energy density.

III. SOUND-LIKE WAVES IN CLASSICAL LATTICE

In quantum mechanics the ground state (quantum vacuum) has finite energy, while in the classical case the vacuum is the state with zero energy. As the lattice we consider is strongly nonlinear, there are no linear modes (sound waves) in the classical system at low energy (therefore it is often called "sonic vacuum"). However, it is possible to have sound-like waves in the classical state with *finite energy density*. These modes can be interpreted as oscillations of the averaged density of a turbulent (chaotic) lattice state. These waves should not be confused with linear waves that appear in the lattice if it is restrained (i.e., if the static positions x_k are nonzero). To find these modes, we simulated numerically the dynamics of classical system (1) at $n = 4$, $\alpha = 1$ with the periodic boundary conditions (another method for the characterization of these modes based on the power spectrum of chaotic dynamics was used in Refs. [6,7]). The simulations are done with a Runge-Kutta-Nystrom method with time step 0.02. Initially a random distribution of momenta p_l is seeded, so that the total energy density per particle is one (because of the scaling properties of the Hamiltonian (1), changing the energy density is equivalent to time rescaling). After a transient of time $T_{\text{trans}} = 10$ a chaotic regime establishes in the lattice. At this time instant we add a perturbation of the form $x_l \rightarrow x_l + \varepsilon \cos ql$ to this chaotic state, with $\varepsilon = 0.1$. The wave number q is changed in the range $0 < q < \pi$. The spatial spectrum of the field x_l contains now, together with a continuous part, a discrete peak at q . We calculated the time evolution of the amplitude f_q of this mode and found, by averaging over the large ensemble, that it varies in time approximately as $f_q \propto e^{-\gamma_q t} \cos \omega_q t$. We use up to 10^7 particles in an ensemble to obtain good averaging of statistical fluctuations.

The numerical results are shown in Fig. 1 for the spectrum of sound-like waves $\omega(q)$ and their decay rates $\gamma(q)$. The frequency spectrum is close to the spectrum of sound in a harmonic lattice $\omega(q) = 2\bar{\omega} \sin q/2$, with $\bar{\omega} \approx 1.4$ (to be compared with value 1.34 obtained in Ref. [7]). At small q we have the spectrum of sound-like waves. Upscaling these results to the arbitrary average energy per particle, we find

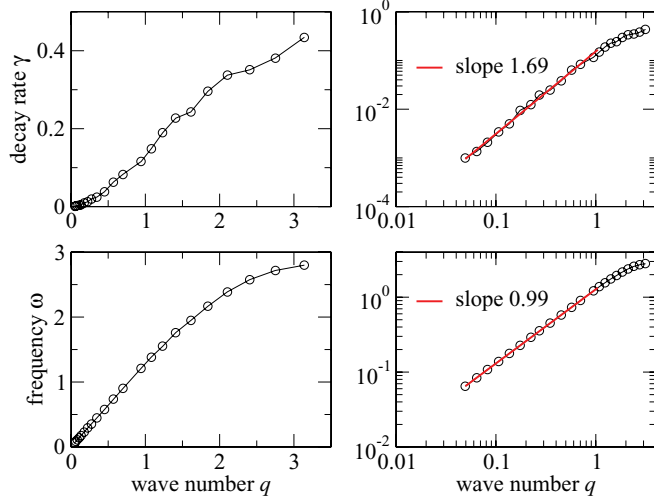


FIG. 1. (Color online) Bottom panels: Spectrum of waves $\omega(q)$ in the classical strongly nonlinear lattice (1) at $n = 4$, $\alpha = 1$ and energy per particle $\langle E_l \rangle$ equal to unity, at small wave numbers q the spectrum is close to a linear law of sound waves $\omega \propto q$. Top panels: Decay rate of sound waves $\gamma(q)$, at small q we have $\gamma \propto q^\beta$ with $\beta \approx 1.69$. Left panels are in normal scale, right panels are in log-log scale, fits are shown by straight lines with indicated slopes.

that the effective velocity of “sound” for these phonon-like excitations is given by $\bar{\omega} \approx 1.4\langle\alpha E_l\rangle^{1/4}$. Here the dependence on a given average energy per particle $\langle E_l \rangle$ appears since a typical frequency of particle oscillations is proportional to $\langle E_l \rangle^{1/4}$. The speed of sound in the physical lattice with distance a between particles is $c = \bar{\omega}a$. The decay rate of these waves drops algebraically with the decrease of the wave vector q as $\gamma \propto q^\beta$. We obtain the value $\beta \approx 1.69$ that is close to the generic exponent $\beta = 5/3$ for the decay rate in nonlinear lattices (see, e.g., Ref. [3]) and corresponds nicely to the value 1.677 obtained in Ref. [7]. Thus even if the dynamics inside the strongly nonlinear lattice is strongly chaotic (see Ref. [18]), the long wave oscillation properties of the average perturbations in the whole lattice are well described by effective sound waves. In a certain sense the situation is similar to sound in a gas media: each particle moves chaotically, but the collective long wave excitations are well described by weakly damping regular sound waves.

We stress that the sound-like waves described in this section are small perturbations of a state with finite energy. We studied their properties in the limit when the amplitude of these waves is very small, and found that the properties do not depend on this amplitude, in this sense these waves can be considered as linear ones. However, they are, of course, not linear waves of the lattice (these do not exist because the lattice is strongly nonlinear), but linear perturbations of a turbulent state having finite energy. Thus their properties depend on this energy, the latter not to be confused with the amplitude of the waves.

It is interesting to note that recently a localization of sound waves in a random three-dimensional elastic network of metallic balls has been observed experimentally in Ref. [31]. Such a system can be viewed as a random three-dimensional ‘Newton’s cradle.’. However, our studies here are restricted to the one-dimensional case.

IV. SIMPLE ESTIMATES FOR QUANTUM STRONGLY NONLINEAR CHAINS

The results of the previous section indicate that the lattice with finite energy density possesses sound-like waves. We can estimate the properties of these waves based on the following relations. The sound velocity c in a gas is given by the derivative of pressure p over the gas mass density ρ at fixed entropy S (adiabatic process): $c^2 = (\frac{\partial p}{\partial \rho})_S$. Since the pressure is proportional to the force $p \propto \partial U / \partial x_l$, hence $c^2 \propto \partial^2 U / \partial^2 x_l$. This leads to a simple estimate for the sound velocity based on the virial theorem according to which $2\langle K \rangle = n\langle U \rangle$, where K and U are the particle kinetic and potential energies and the brackets mark their average values. Since the temperature is proportional to the kinetic energy we have $T \sim \langle K \rangle = n\langle U \rangle = \alpha\langle(x_i - x_j)^n\rangle \sim \alpha(\Delta x)^n$ where Δx is an average displacement of a particle. This gives

$$c^2 = \omega^2 a^2 \sim a^2 U''(\Delta x) \sim a^2 \alpha^{2/n} T^{1-2/n}. \quad (7)$$

For the classical case this expression agrees with the previous analytical results for $\bar{\omega}$ for $n = 2, 4$. We stress again that velocity (7) refers to the velocity of small perturbations on the base of a turbulent state having finite energy. Thus this velocity does depend on this energy, but does not depend on the amplitude of small perturbations.

Next we are going to perform similar estimations for the vacuum state in the quantum lattice. For the quantum strongly chain we can use the Heisenberg uncertainty relation $p \sim \hbar/\Delta x$ for the minimization of the ground-state energy $E = \hbar^2/2(\Delta x)^2 + \alpha(\Delta x)^n/n$ that gives $\Delta x \sim (\hbar^2/\alpha)^{1/(n+2)}$. Now we estimate frequency ω as the frequency of oscillations in the potential $U(x) \sim x^n$ that have the amplitude Δx : $\omega^2 \sim \alpha(\Delta x)^{n-2} = \alpha^{4/(n+2)}\hbar^{2(n-2)/(n+2)}$. As a result, using the relation $c^2 = \omega^2 a^2$, the sound velocity of the quantum chain can be estimated as

$$c^2 \sim a^2 \alpha^{4/(n+2)} \hbar^{2(n-2)/(n+2)}. \quad (8)$$

For $n = 2$ this velocity is independent of \hbar and coincides with the velocity of sound waves, but for $n > 2$ it decreases with \hbar that corresponds to the decrease of the ground-state energy of a nonlinear oscillator.

V. NUMERICAL RESULTS OF QUANTUM MONTE CARLO

A. Method description

For our numerical simulations of quantum chain (1) we use the Metropolis algorithm (MA) [32] in the Euclidean time τ related to the system temperature $T = \hbar/\tau$. The simulations are done in the same way as for the studies of the quantum Frenkel-Kontorova model described in Ref. [20]. A general description of this QMC method can be found in [33].

The paths in the discretized Euclidean time are generated by the statistical sum

$$\sum_{\{x_{l,j}\}} \exp \left[- \sum_{l,j} [(x_{l,j} - x_{l,j-1})^2 / 2\Delta\tau + \Delta\tau(x_{l,j} - x_{l-1,j})^n / 2n] \right], \quad (9)$$

which links the problem to a statistical mechanics for the configuration distribution of some lattice of size $N \times N_\tau$, where N is the number of particles and $N_\tau = \tau/\Delta\tau$ is the number of discrete steps of size $\Delta\tau$ in the Euclidean time interval τ . As usual the periodic boundary conditions are used in this time with $x_l(\tau_j + \tau) = x_l(\tau_j)$ and $\tau_j = j\Delta\tau$. In our numerical studies we use up to $N_\tau = 1000$, $\tau = 200$ and up to $2 \cdot 10^6$ Metropolis updates. We fix $\alpha = 1$ for numerical simulations.

The numerical simulations generate configurations $\{x_{k,j}\}$ with a probability proportional to their weights in the partition function. The Metropolis method looks very efficient, providing an update step gives rather large modifications for a given site. However, the corresponding modifications are local and are dominated by the nearest-neighbor sites that result in a significant slowdown for long wave configurations. Thus it is useful to combine the Metropolis method with the microcanonic dynamics (MCD) method. The MCD method is a noiseless algorithm and it works as follows: All variables $x_{l,m}$ are considered as some coordinates, and the sum

$$\sum_{l,j} \left[\frac{1}{2\Delta\tau} (x_{l,j} - x_{l,j-1})^2 + \frac{\Delta\tau}{2n} (x_{l,j} - x_{l-1,j})^n \right] \equiv \mathcal{U}(x), \quad (10)$$

as a potential energy of a certain system. Then, a set of auxiliary momentum variables $\{\mathcal{P}_{l,j}\}$ is added and the equations of motion are solved numerically in an auxiliary update “time” variable u

$$\begin{aligned} \partial \mathcal{P}_{l,j} / \partial u &= -\frac{\partial \mathcal{U}}{\partial x_{l,j}} = \nabla_{l,j} \mathcal{U}(x), \\ \partial x_{l,j} / \partial u &= \mathcal{P}_{l,j}. \end{aligned} \quad (11)$$

With this dynamical description the system evolves over some iso-energy hypersurface in the phase space, and we get an ensemble of configurations.

However, an obvious disadvantage of such a method is that one needs to solve the differential equations numerically with a step which becomes smaller for decreasing $\Delta\tau$ due to the terms $\mathcal{U}(x)$ with $\Delta\tau$ in the denominator. But even worse, these terms act as some noise that reduces the relaxation rate along l (space dimension). Thus, to accelerate the relaxation processes we introduce into $\mathcal{U}(x)$ a parameter C_K

$$\begin{aligned} \mathcal{U}(x; C_K) &= \sum_{l,j} \left[\frac{C_K}{2\Delta\tau} (x_{l,j} - x_{l,j-1})^2 \right. \\ &\quad \left. + \frac{\Delta\tau}{2n} (x_{l,j} - x_{l-1,j})^n \right]. \end{aligned} \quad (12)$$

Then the update step is organized as follows:

- (a) the fast mixing stage, with $C_K = \Delta\tau$, at which the smallness of denominator is canceled, here the MCD method is applied during the auxiliary “time” interval $u \sim 100$;
- (b) return to $C_K = 1$ and application of the Metropolis updates at maximum 400 updates.

Such a combined approach allows us to reduce significantly the required number of Metropolis updates needed to get a next configuration. This allows us to have more rapid numerical simulations. We checked that both methods (only the MA steps

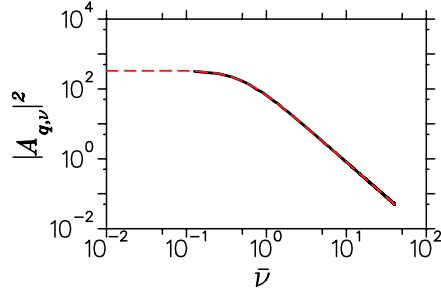


FIG. 2. (Color online) Typical data for the Fourier harmonics $|A_{q_j, v_m}|^2$ and its fit by the dependence (14); the black curve shows numerical data, dashed red/gray curve shows the fit (curves are overlapped). Data correspond to the linear chain at $n = 2$, $\hbar = 1$, $q_j = 10\pi/N$, $N = 64$, $\tau_{\max} = 100$, $N_\tau = 1000$.

and MA steps combined with the MCD method) converge to the same results.

B. Quantum excitations above the quantum vacuum

The ensemble of quantum paths, obtained by the numerical methods described previously, can be used to determine the properties of the quantum vacuum ground state of the system and of the excitations above it. The averages of various quantities over this ensemble give the corresponding expectation values at the ground state. However, the study of fluctuations of quantum paths allows us to extract a more interesting information about the spectrum of low-energy elementary excitations above the quantum vacuum.

To extract this information we use the approach of the authors of Ref. [20] and consider the Fourier harmonics of quantum paths

$$A_{q_j, v_m} = \sum_{l,k} x_{l,k} \sin(q_j l) \exp(i v_m \tau_k), \quad (13)$$

where $q_j = \pi j/N$, $j = 1, \dots, N-1$, $\tau_k = k\Delta\tau$, $v_m = 2\pi m/\tau_{\max}$, $m = 0, \dots, N_\tau/2$. One expects a Lorentzian distribution in frequency ω for the exponential decay of quasiparticle excitations in the imaginary time

$$\langle |A_{q_j, v_m}|^2 \rangle = \frac{\hbar}{2} \frac{1}{\omega^2 + \bar{v}_m^2}. \quad (14)$$

Here we use the renormalized frequency $\bar{v}_m = \frac{2}{\Delta\tau} \sin(v_m \Delta\tau/2)$ with the sine term appearing due to the discreteness of time steps. The fit of data for A_{q_j, v_m} allows us to find the spectral dependence $\omega = \omega(q_j)$ and thus to determine the dispersion law of elementary quantum excitations. A typical example of such a fit is shown in Fig. 2.

The spectrum of low-energy excitations extracted via such a procedure is shown in Fig. 3 for $n = 2, 4, 8$. For $n = 2$ the data reproduce the theoretical result for a harmonic chain with $\bar{\omega} = \omega(q)/[2 \sin(q/2)] = 1$. For $n = 4, 8$ this form of the spectrum is preserved with a moderate renormalization of $\bar{\omega} \approx 1.2, 1.5$, respectively. This shows that even if the classical strongly nonlinear chain is fully chaotic the quantum vacuum is rather regular and is characterized by the phonon-type excitations rather similar to the case of a harmonic chain. Although this was pre-assumed in estimations leading to Eq. (8), without the numerical evidence of Fig. 3 this equation would be useless.

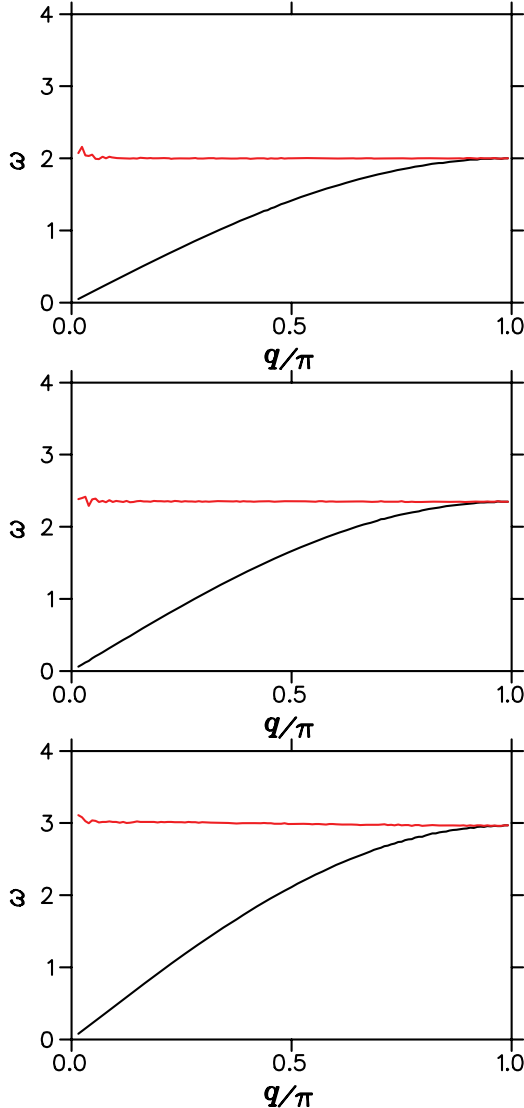


FIG. 3. (Color online) Spectra of quantum phonon modes shown by the black bottom curve and obtained from QMC simulations for (top panel) $n = 2$, (middle panel) $n = 4$, and (bottom panel) $n = 8$; top red/gray curve shows the ratio $\omega/\sin(q/2)$ for each panel. The data are obtained at $\hbar = 1$, $N = 128$, $N_\tau = 1000$, $\tau_{\max} = 200$, the simulations are done with the MA using $2 \cdot 10^6$ updates.

Our data show that $\bar{\omega}$ varies with \hbar and n . This leads to the dependence of the sound velocity $c = d\omega/dq$ on these two parameters. The numerically obtained dependence of c on \hbar is shown in Fig. 4. The fit by an algebraic dependence $c \propto \hbar^\eta$ gives $\eta = 0.33; 0.56$ for $n = 4, 8$, respectively. These numerical values are close to the theoretical power from Eq. (8) with $\eta = (n - 2)/(n + 2)$ corresponding to $\eta = 1/3, 3/5$ for these n values. The global variation of the whole spectrum $\omega(q)$ with \hbar is shown in Fig. 5 for $n = 4$.

Trying to find deviations from a harmonic chain behavior we compute numerically the amplitudes of phonon modes S_q^2 [see Eq. (3) with $q = k/(N - 1)$] and the correlation function $\langle x_l x_{l+\Delta} \rangle_l$ [see Eq. (4)]. The results are shown in Fig. 6. For $n = 2$ the numerical data are in good agreement with the theory for a harmonic chain. For $n = 4, 8$ our numerical data show the dependencies rather similar to the case of a harmonic

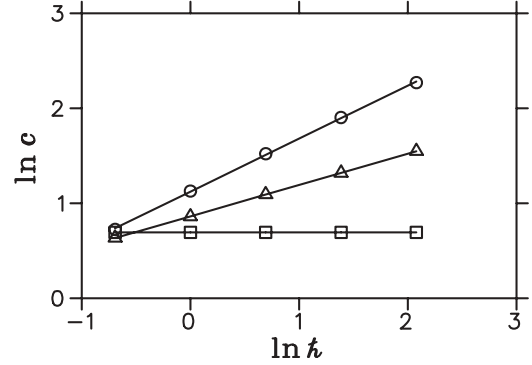


FIG. 4. The dependence of sound velocity c on \hbar . Squares, triangles, and circles correspond to $n = 2, 4$, and 8 , respectively. The straight lines show the fit dependence (see text). Parameters of simulations are $N = 64$, $\tau_{\max} = 100$, and $N_\tau = 1000$. Logarithms are natural.

chain with slight vertical shift, which can be attributed to the modified values of $\bar{\omega}$ discussed previously. We note that for the case of $T > 0$ the theoretical formulas (3) and (4) are computed with the expression (5) for bosonic excitations at finite temperature. Since the value of τ in Fig. 6 is rather large there is no significant difference between the theoretical expressions for $T = 0$ and $T = \hbar/\tau$.

An additional attempt to see deviations from a harmonic chain behavior is performed by computing the form factor $F(q)$ of the chain given by Eq. (6). However, the results presented in the left panel of Fig. 7 show that all three chains with $n = 2, 4, 8$ give very similar curves for $F(q)$ which practically overlap.

The confirmation of similarity between these three types of chains in the ground state is given by the direct computation of the correlator $K(q_1, q_2) \equiv \langle S_q S_{q'} \rangle / (\langle S_q S_q \rangle \langle S_{q'} S_{q'} \rangle)^{1/2}$ which should be proportional to δ_{q_1, q_2} according to Eq. (3). Indeed, the numerical data show a strong peak at $q_1 = q_2$ with a residual noisy level of K at other $q_1 \neq q_2$ without any structural dependence on q_1, q_2 . This residual level can be characterized

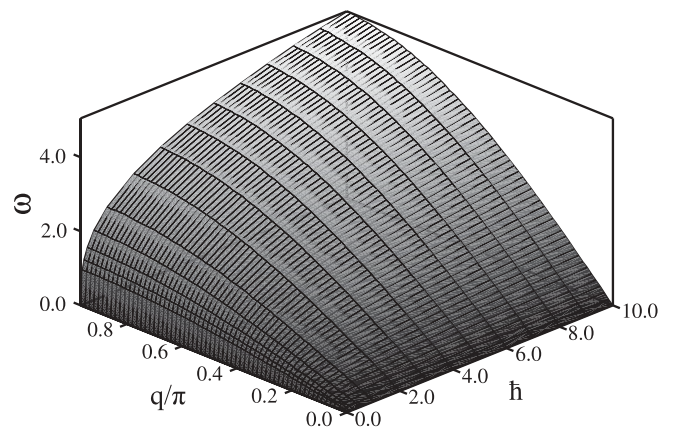


FIG. 5. Spectra of quantum phonon modes for the quartic chain at $n = 4$. Data correspond to $N = 64$, $\tau = 100$, $N_\tau = 1000$, and to the interval $\hbar = 0.063 - 10$, extrapolated smoothly from $\hbar = 0.063$ to $\hbar = 0$.

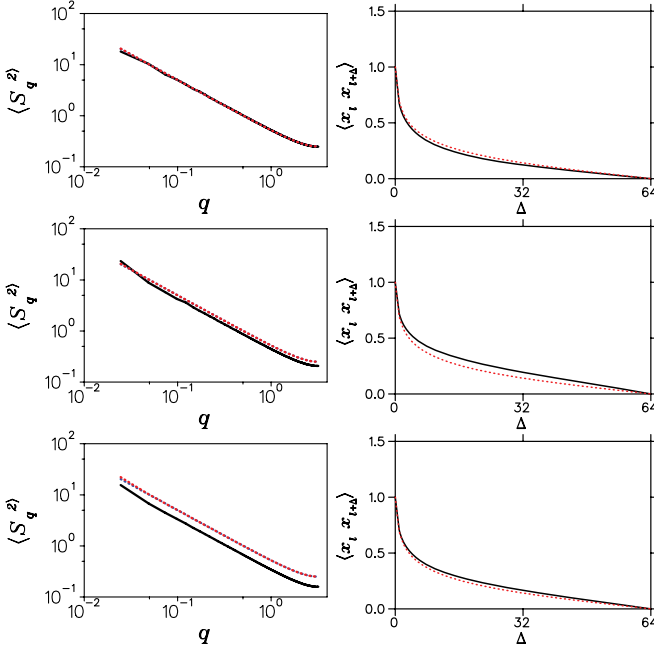


FIG. 6. (Color online) Left column: Amplitudes of phonon modes, see Eq. (3), for (top) $n = 2$, (middle) 4, and (bottom) 8. Right column: Normalized correlation function, see Eq. (4), for $l = 64$ (central particle) for the same order of panels. Other parameters $\hbar = 1$, $N = 128$, $N_\tau = 1000$, and $\tau = 200$. Simulations include $2 \cdot 10^6$ updates. Red/gray and blue/black dotted curves give the theoretical expectations for harmonic chain with temperature $T = \hbar/\tau$ and $T = 0$, respectively (curves overlap).

by the total weighted admixture of other modes to a given mode q via

$$w(q) = \sum_{q' \neq q} |\langle S_q S_{q'} \rangle|^2 / |\langle S_q S_q \rangle|^2. \quad (15)$$

This characteristic is shown in the right panel of Fig. 7 for $n = 2, 4, 8$. The admixture $w(q)$ increases with n , but still it remains rather small for strongly nonlinear lattices with $n = 4, 8$. This gives one more confirmation that the quantum vacuum is rather close to a harmonic one.

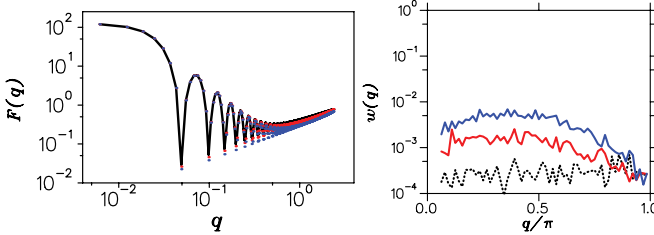


FIG. 7. (Color online) Left panel: Form factor $F(q)$, see Eq. (6), for $n = 2$ (black curve), 4 (red/gray points), 8 (blue/black points) (data practically coincide). Other parameters are as in Fig. 6 including $\alpha = 1$. Right panel: Admixture to normal modes from other harmonics. Red/gray and blue/black curves show data for quartic and octic chains, the dotted black curve corresponds to the linear chain and gives an estimate for a noise level. Data correspond to $\hbar = 1$, $N = 64$, $\tau = 50$, and $N_\tau = 500$ and the number of independent quantum paths is 10^4 .

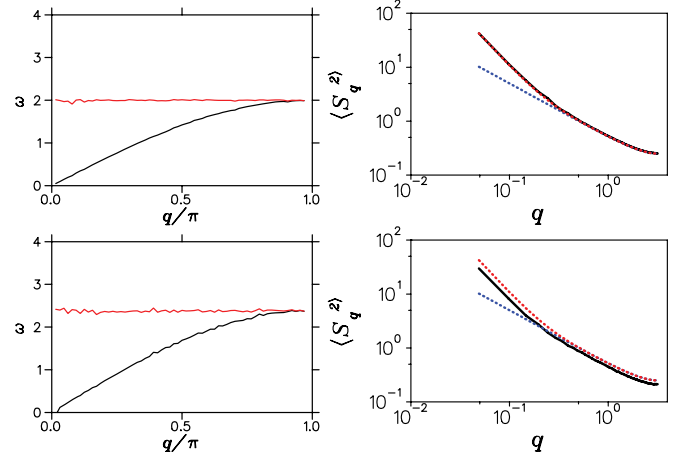


FIG. 8. (Color online) Left column: Spectra of quantum phonon modes at $T = 0.1$ for $n = 2$ (top) and 4 (bottom) with the curves as in Fig. 3. Right column: Amplitudes of phonon modes, see Eq. (3) in the same order; red/gray and blue/black dotted lines give theoretical expectations for harmonic chain with temperature $T = \hbar/\tau$ and $T = 0$, respectively. Other parameters are $\hbar = 1$, $N_\tau = 200$, $\tau_{\max} = 10$. Simulations are done with the combined MA and MCD method with 10^4 Metropolis updates.

At finite temperatures the spectrum of excitations $\omega(q)$ and the amplitudes of phonon modes S_s^2 are still well approximated by the theoretical dependence for a harmonic chain as it is shown in Fig. 8 at $T = 0.1$ which is about two times larger than the excitation energy for a mode with minimal frequency $\hbar\omega_{\min} = \hbar\pi/N \approx 0.049$. The situation is found to be qualitatively the same when the temperature is increased up to $T = 1$ keeping fixed other parameters of Fig. 8 even if at $n = 8$ the splitting between the theoretical curve and the numerical data becomes more visible (due to the similarity of these data with Fig. 8 we do not show them here).

VI. SUMMARY

In this work we investigated the properties of collective modes in strongly nonlinear chains. For the classical chains we find that the chain has sound-like modes which decay rather slowly due to nonlinear wave interactions with the rate $\gamma \propto q^\beta$ with $\beta \approx 5/3$. This decay rate is in agreement with the generic result of the decay of sound waves in one-dimensional weakly nonlinear chains [3].

On local scales the classical dynamics in such strongly nonlinear chains is strongly chaotic. One could expect that this chaos may lead to nontrivial properties of quantized chains. However, our extensive numerical studies of a quantum vacuum show that it is characterized by low-energy phonon excitations which are rather similar to those of a harmonic chain. The main difference is that the sound velocity of these phonon modes depends on a dimensionless Planck constant as it is described by Eq. (8).

In a certain sense quantum effects suppress the signatures of classical chaos in the ground state. Such a phenomenon is known for quantum systems with a few degrees of freedom. For example, a ground state of a Sinai billiard can be rather well approximated by a Hartree-Fock trial function with one

maximum so that the signatures of quantum chaos appear only in the semiclassical regime for highly excited states [34]. This is more or less natural for systems with few degrees of freedom. Our case has an infinite number of degrees of freedom, but in spite of that the quantum vacuum remains rather similar to a quantum vacuum of a harmonic chain in which the oscillator frequency is dependent of an dimensionless Planck constant. It is possible that certain signatures of such quasi-integrability at low energies find their manifestations in a slow chaotization of excitations in a quantum Newton's cradle observed in the experiments [21]. However, we should note that such a statement can be considered only on a qualitative level of rigor since the model (1) at $n = 4$ or 8 gives only an approximate description of ball interactions (see discussion in Ref. [18]).

It is possible that a degeneracy of chaos in the vicinity of a quantum vacuum is linked to the space homogeneity of the model (1). Indeed, the ground state of the quantum Frenkel-Kontorova model has many more rich properties [20] appearing due to the presence of a periodic potential.

In this paper we have applied methods that are well adapted for the analysis of low-energy oscillatory quantum waves. It is possible that other approaches should be used to detect quantum-shockwave-type excitations with large displacements between two parts of the chain (in principle, the energy of such a type compacton-like excitations is not very high and is independent of the lattice size). One approach allowing us to study the quantum coherence of discrete kink solitons in quasi-one-dimensional ion traps has been very recently pursued in Refs. [26,27]. We expect that the quantum vacuum described in our paper is an essential ingredient of the dynamics in such experimental setups.

ACKNOWLEDGMENTS

One of us (OVZ) is supported by the RAS joint scientific program “Fundamental problems in nonlinear dynamics” and thanks UMR 5152 du CNRS, Toulouse for hospitality during this work, another (DLS) thanks the University of Potsdam for hospitality at the final stage of this work.

-
- [1] E. Fermi, J. Pasta, S. Ulam, and M. Tsingou, Los Alamos Report LA-1940 (1955); E. Fermi, *Collected Papers* (University of Chicago Press, Chicago, 1965), Vol. 2, p. 978.
 - [2] S. Flach and C. R. Willis, *Phys. Rep.* **295**, 181 (1998).
 - [3] S. Lepri, R. Livi, and A. Politi, *Phys. Rep.* **377**, 1 (2003).
 - [4] *The Fermi-Pasta-Ulam Problem: A Status Report*, edited by G. Gallavotti, (Springer, Berlin, 2007).
 - [5] T. Dauxois and S. Ruffo, [http://www.scholarpedia.org/article/Fermi-Pasta-Ulam_nonlinear_lattice_oscillations].
 - [6] C. Alabiso and M. Casartelli, *J. Phys. A: Math. Gen.* **34**, 1223 (2001).
 - [7] S. Lepri, R. Livi, and A. Politi, *CHAOS* **15**, 015118 (2005).
 - [8] V. F. Nesterenko, *J. Appl. Mech. Tech.* **24**, 733 (1983).
 - [9] C. Coste, E. Falcon, and S. Fauve, *Phys. Rev. E* **56**, 6104 (1997).
 - [10] A. Chatterjee, *Phys. Rev. E* **59**, 5912 (1999).
 - [11] M. A. Porter, C. Daraio, E. B. Herbold, I. Szelengowicz, and P. G. Kevrekidis, *Phys. Rev. E* **77**, 015601(R) (2008).
 - [12] A. N. Lazaridi and V. F. Nesterenko, *J. Appl. Mech. Tech. Phys.* **26**, 405 (1985).
 - [13] S. L. Gavrilyuk and V. F. Nesterenko, *J. Appl. Mech. Tech. Phys.* **34**, 784 (1994).
 - [14] V. Nesterenko, *Dynamics of Heterogeneous Materials* (Springer, New York, 2001).
 - [15] D. Novoa, B. A. Malomed, H. Michinel, and V. M. Pérez-García, *Phys. Rev. Lett.* **101**, 144101 (2008).
 - [16] P. Rosenau and J. M. Hyman, *Phys. Rev. Lett.* **70**, 564 (1993).
 - [17] P. Rosenau, *Phys. Rev. Lett.* **73**, 1737 (1994).
 - [18] K. Ahnert and A. Pikovsky, *Phys. Rev. E* **79**, 026209 (2009).
 - [19] S. Sen, J. Hong, J. Bang, E. Avalos, and R. Donev, *Phys. Rep.* **462**, 21 (2008).
 - [20] O. V. Zhirov, G. Casati, and D. L. Shepelyansky, *Phys. Rev. E* **67**, 056209 (2003).
 - [21] T. Kinoshita, T. Wenger, and D. S. Weiss, *Nature (London)* **440**, 900 (2006).
 - [22] V. A. Yurovsky, M. Olshanii, and D. S. Weiss, *Adv. At. Mol. Opt. Phys.* **55**, 61 (2008).
 - [23] M. C. Gutzwiller, *Chaos in Classical and Quantum Mechanics* (Springer, New York, 1990).
 - [24] L. S. Schulman, *Phys. Rev. A* **68**, 052109 (2003).
 - [25] V. V. Konotop and S. Takeno, *Phys. Rev. E* **63**, 066606 (2001).
 - [26] H. Landa, S. Marcovitch, A. Retzker, M. B. Plenio, and B. Reznik, *Phys. Rev. Lett.* **104**, 043004 (2010).
 - [27] A. del Campo, G. De Chiara, G. Morigi, M. B. Plenio, and A. Retzker, *Phys. Rev. Lett.* **105**, 075701 (2010).
 - [28] G. J. Milburn, [arXiv:quant-ph/9908037](http://arxiv.org/abs/quant-ph/9908037).
 - [29] R. Lifshitz and M. C. Cross, *Reviews of Nonlinear Dynamics and Complexity*, edited by H. G. Shuster (Wiley, New York, 2008), Vol. 1, p. 52.
 - [30] A. D. O'Connell *et al.*, *Nature (London)* **464**, 697 (2010).
 - [31] H. Hu, A. Strybulevych, J. H. Page, S. E. Skipetrov, and B. A. van Tiggelen, *Nature Physics* **4**, 945 (2008).
 - [32] N. Metropolis, A. Rosenbluth, M. Rosenbluth, A. Teller, and E. Teller, *J. Chem. Phys.* **21**, 1087 (1953).
 - [33] S. L. Sondhi, S. M. Girvin, J. P. Cai, and D. Shahar, *Rev. Mod. Phys.* **69**, 315 (1997).
 - [34] F. Haake, *Quantum Signatures of Chaos* (Springer, Berlin, 2001).